POAC'15
Trondheim, Norway

Proceedings of the 23rd International Conference on
Port and Ocean Engineering under Arctic Conditions
June 14-18, 2015
Trondheim, Norway

CHARACTERIZATION OF HAZARDOUS ICE USING RADARSAT-2 AND ICE PROFILING SONAR

K. Ersahin[1], L. Brown[1], R. Kerr[1], M. Henley[1], L. Sadava[1], E. Ross[1], T. Mudge[1], D. Fissel[1]

ASL Environmental Sciences Inc.[1]

ABSTRACT

Ice can pose a hazard for operations (e.g., transportation, shipping, surveillance, offshore oil and gas exploration) and for infrastructure (e.g., ports, pipelines, offshore structures). There is an increasing need for fine-scale characterization of hazardous ice conditions. This information is of interest to many stakeholders including industry and government agencies. Spaceborne SAR sensors are being used for near-real-time monitoring of the regional ice conditions. Satellite-derived sea ice information products typically rely on the interpretation of ice analysts, sometimes supported by semi-automated tools. However, validation of data products remains a challenge due to limited or no *ground truth*.

Operated from subsurface moorings located below the sea ice canopy, the ULS instrumentation, consisting of the ASL Ice Profiling Sonar (IPS) and the Acoustic Doppler Current Profiler (ADCP), provides accurate measurements of ice draft on a continuous basis and allow detailed characterization of potentially hazardous ice features, e.g., large keels, hummocky ice, multi-year ice, episodes of large internal ice pressures, and glacial ice.

In this work, our objective was to calibrate and validate satellite-based ice data products using continuous measurements obtained from ULS instruments. We focused on the development of techniques to integrate high resolution polarimetric RADARSAT-2 imagery and corresponding ULS datasets to characterize hazardous ice. The results include paired satellite and ULS datasets; calibration and validation of algorithms for hazardous ice detection and satellite-based ice draft estimation.

INTRODUCTION

The areal coverage of Arctic marine ice is now rapidly reducing in summer, changing the ecosystem of the region, altering the use of marine areas by indigenous peoples and greatly increasing shipping access to the area. In spite of the reductions in ice cover, navigation in Arctic areas is perilous, and there are important and dangerous ice hazards in the form of dense multi-year ice, large individual ice keels, fields of hummocky ice, and regions of high internal ice pressure. With the evolving Arctic ice regime the likelihood and impact of interactions with these ice hazards are likely to also change. There is a critical need for improved understanding of the marine ice regime in the form of:

- Improved knowledge of the properties of marine ice for input to engineering design of coastal and offshore platforms and as inputs to Arctic ship design;
- Informing the development of government policies required for regulation of Arctic shipping, regulating energy development, marine uses of the area and others;
- Operational support for shipping and industry activities;
- Improved characterization of sea ice as an important part of ecosystem understanding required for environmental assessments and the regulatory approval process.

Measurements of ice draft obtained using moored Upward Looking Sonar (ULS) instruments have a horizontal resolution and vertical thickness accuracy which exceed the performance of other advanced ice measurement methods (Fissel and Marko, 2011). Operated from subsurface moorings located below the sea ice canopy, the ULS instrumentation, consisting of the ASL Ice Profiler Sonar (IPS) and the Acoustic Doppler Current Profiler (ADCP) are deployed 25 to 60 m below the air-water interface from seafloor-based moorings, or in shallower water, at near-bottom moorings. ULS instruments provide accurate measurements of ice draft on a continuous year-long basis and allow detailed characterization of keel shapes and other ice features (Fissel *et al*., 2008). High resolution ice thickness and velocity information can be obtained along thousands of kilometers of ice which move over the mooring locations through the ice season. These measurements provide important data for establishing met-ocean design criteria related to oil and gas operations in areas with seasonal or year-round ice cover. The methods developed in detailed processing and analysis of ULS data sets have led to quantitative characterizations of potentially hazardous ice features (Fissel *et al*., 2012), in the form of large individual ice keels, segments of large hummocky (rubbled) ice, multi-year ice features, episodes of large internal ice pressures, and glacial ice features.

Spaceborne Synthetic Aperture Radar (SAR) sensors are ideal for sea ice monitoring because of their all-weather operation and sensitivity to surface roughness. Although operational requirements for ice monitoring programs typically rely on wide area coverage (e.g., 300-500 km swath width), there is also a need for fine scale characterization of potentially hazardous ice conditions. The information provided by polarimetric SAR (e.g., RADARSAT-2 quad-pol) datasets is expected to improve the ability to characterize targets through their scattering properties, at the expense of reduced coverage (25-50 km). The next generation Canadian spaceborne radar system, i.e., RADARSAT Constellation Mission (RCM), will have new beam modes with compact polarization (CP) capability. This will provide increased information content over the wide coverage of dual-polarized systems. Thus, more frequent and wide area coverage of these data will enhance the near real time monitoring of sea ice.

The ULS data *view from below* and SAR data *view from above* provide complementary information sources where utilizing both is expected to result in better characterization of the ice conditions. This concept is illustrated in Figure 1, where independent measurements of the ice conditions could also help to validate existing data analysis and interpretation methods from either source. As a result, existing capabilities for detection and characterization of hazardous ice features will be enhanced. The results will demonstrate value to various stakeholders including government departments and agencies, and the oil and gas and shipping industries.

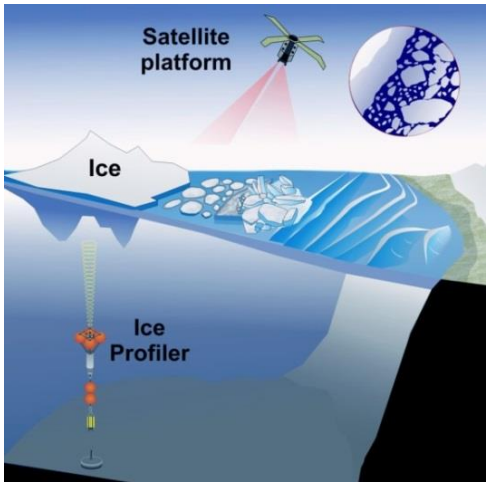

Figure 1. An illustration of combining the views from above (satellite) and below (ULS).

METHODOLOGY

In this section, our methodology is described, starting from the data acquisition and assembly for both ULS and satellite datasets. Then, ice characterization and hazardous ice feature detection from ULS data is discussed, followed by the methods used to combine RADARSAT and ULS datasets. Finally, we introduce the algorithms used for satellite-based sea ice characterization and comparison with ULS results.

Data Acquisition and Assembly

Data acquisition and assembly involved two main data sources (i.e., ULS and spaceborne SAR). Since simultaneous collection of these datasets is necessary, we first utilized the archived ULS datasets (owned by research organizations and the oil and gas industry), where matching high resolution quad-polarized RADARSAT-2 data was available. These data were from 2011 summer in the Chukchi and Beaufort Seas. Then, for the ULS moorings that were collecting data in 2013-14, an assessment of expected hazardous ice types, location, and accessibility was performed. As a result, RADARSAT-2 was tasked for new data acquisitions and collected data using Fine Quad (FQ) beam modes in the early winter (Dec–Jan) and summer (May-Jun) for a number of sites in the Chukchi, the Beaufort, NE Baffin Bay, NE Greenland, and the Barents Sea.

Ice Characterization from ULS data

The ASL Ice Profiling Sonar (IPS) measures a suite of parameters that are used to determine the draft of the overhead ice canopy including the return time of travel for acoustic pings from the IPS sonar transducer to a target. The pressure at the instrument depth, the tilt of the instrument, and the temperature are also used to derive an *ice draft time series*, where variations in the speed of sound over the IPS deployment are accounted for during data processing. The horizontal extent of the ice draft is at this point is not determined. By combining the ice draft with the ice velocity time series obtained from the Acoustic Doppler Current Profiler (ADCP), both the vertical and horizontal spatial dimensions can be determined. The result is an *ice draft spatial series*.

The ice draft spatial series and other supporting met-ocean data are analyzed using the methodologies and tools for quantitative characterizations of potentially hazardous ice features, in the form of large individual ice keels, segments of large hummocky (rubbled) ice, multi-year ice (Fissel *et al*., 2012). Identification and characterization of large keels (i.e. deep and/or wide) is performed with a feature detection software tool operated on an ice draft spatial series. An analogous tool is used to detect hummocky ice features. Individual large ice keels have the largest ice thickness of 8 m or more while large hummocky ice features have greater horizontal scales of 100 to several hundred meters with smaller ice thickness. Multi-year ice detection algorithm is based on the analysis of the backscatter profile at the ice-water interface (Fissel *et al*., 2012).

The characterizations obtained from the analysis of ULS datasets are reported together with the ice draft spatial series for a period of interest that typically represents a short segment corresponding to an image dataset.

Combining ULS and RADARSAT Datasets

The spatial-temporal correspondence of the ULS and RADARSAT data need to be examined in great detail before using these datasets as complementary sources of information. The view from above (satellite) and the view from below (ULS) measure different physical properties of the ice pack at different spatial and temporal scales. The satellite data over a mooring site is

acquired over a large area within a very short time period, while ULS data represents a single position in space over a much longer period. Depending on the ice velocity this period may be from a few hours to several days. As a result, the two data sets have a varying level of temporal decorrelation that is zero at the mooring location at the image acquisition time.

The drifting ice over the mooring allows us to generate an ice draft spatial series (i.e, IPS track) that can then be overlaid on the satellite image data. The overlay is achieved through the "rigid body" assumption, where over the time period used for the overlay the ice pack is assumed to have spatially coherent motion, or in other words the pack ice has not deformed significantly. The temporal decorrelation is minimum at the mooring location and increases along the IPS track. Any deviation from the rigid body assumption results in spatial decorrelation manifesting itself as a positional error in the apparent IPS track. Accurate georeferencing of satellite imagery and accurate ice velocity especially direction information (requires very good characterization of ADCP compass calibration) are also very important to achieve acceptable co-registration between data sources.

Decorrelation in space and time due to a number of factors limit the amount of data that can be used for validation with high confidence. Therefore, assessment of the *correlation length* between the two data sources is necessary. The first method we use for assessment is called 'drift field' where pairs of RADARSAT images that are closely spaced in time are used to determine the variability in the motion of the ice pack. Ice features that exist in both images are used to generate an ice drift field (Figure 2a). If the drift vectors indicate a coherent motion for the section of IPS track between the two image acquisition times (shown by the yellow and red symbols) then the ice pack is considered to be moving as a 'rigid body'. The second method, 'floe edge', uses readily identifiable segments of open water in a single image to assess spatial correlation with a superimposed IPS track (Figure 2b).

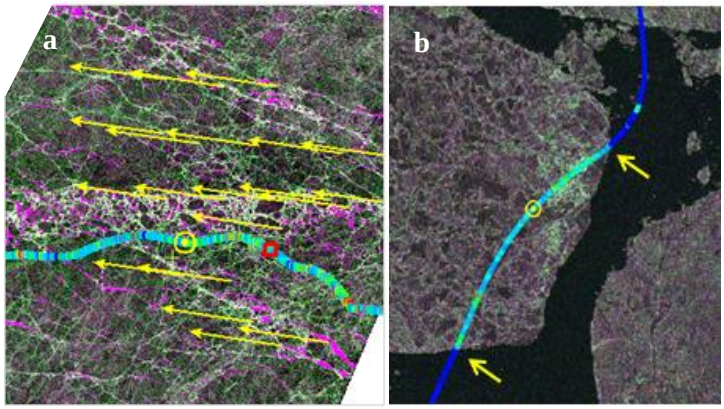

Figure 2. Methods for assessing correlation length. (a) Drift field, (b) Floe edge.

One aspect of correlation length assessment that is not considered by the above methods is the amount of time represented by an IPS track or a pair of RADARSAT images. Depending upon oceanographic and meteorological conditions (air or water temperature, precipitation, etc.); even if the ice drift field is coherent and the spatial correlation between IPS and RADARSAT imagery is strong, *in situ* changes to the ice can result in decorrelation of the features themselves. For example, ice thickness can change over periods of hours under very cold conditions, or conversely under warm conditions melting can occur. For this reason our comparisons of IPS and RADARSAT were generally restricted to offsets of one day or less. For each dataset a record of meteorological conditions was also available to assist with interpretation.

Satellite-based Sea Ice Characterization

This section describes the methodology used to determine if satellite-derived parameters can serve as a proxy for ice draft, and how satellite data may be used to detect hazardous ice (as described by the ULS datasets) for the entire image extent.

In the polarimetric SAR literature, there are a number of techniques that were shown to be promising for classification of sea ice data. These include polarimetric parameters derived from Cloude-Pottier's eigenvalue decomposition (Cloude and Pottier, 1997, Scheuchl *et al*., 2003), Freeman-Durden decomposition (Freeman and Durden, 1998), Touzi decomposition (Touzi, 2007), Yamaguchi decomposition (Yamaguchi, 2005). In addition, a number of polarimetric products tested by Gill and Yackel (2012) and (Gill *et al*., 2013), depolarization factors (Kim *et al*., 2012), and Shannon Entropy (Casey *et al*., 2013) were investigated.

For polarimetric data processing open source software tools (i.e., PolSARPro, RSTB), image processing software packages (i.e., PCI, ENVI), and other custom software developed by ASL were used. First, the Refined Lee speckle filter (7x7) was applied and then polarimetric data products were generated from the filtered coherency matrix. Data processing was followed by the qualitative assessment of visual information in polarimetric image products. Then, the IPS track overlay on polarimetric image products was used to extract the data values from under the track at spatial scales ranging from 5x5m to 350x350m kernels for an image pixel size of 5x5m. IPS draft measurements were similarly averaged along track to matching spatial scales.

A number of quantitative techniques were used to compare satellite and ULS datasets. We first compared the SAR backscatter and other polarimetric products with ice draft, over the range of spatial scales. The intent was to evaluate these products for their ability to estimate ice draft (used as a proxy for thickness). The rationale for making comparisons at different spatial scales was that the surface features (from satellite) and bottom features (from ULS) would not necessarily mirror one another, but would be correlated at some spatial scale.

Our second analysis involved the histograms of polarimetric parameter values for the ice types identified from ULS datasets (e.g., keel, hummocky). We aimed to evaluate the ability of the image products to resolve such ice types. To quantify class separability we performed simple two-tailed t-tests which compared the differences between the means of two classes with their pooled standard deviation. Finally, IPS and RADARSAT classifications were compared to evaluate the extent to which these two techniques extract similar ice characteristics.

RESULTS

Datasets

Among the four datasets analyzed in the Beaufort and Chukchi Seas, only three ULS-based ice types were present (i.e., hummocky ice, deep keels and non-hazardous ice), as well as open water. These datasets did not show a clear multi-year ice (MYI) presence. In this paper, we only present one of the datasets: "IOS site 2". After this paper was written a fifth dataset from NE Greenland that included both first year and multi-year ice was analyzed.

The "IOS site 2" mooring is located on the outer continental shelf in the Canadian Beaufort Sea at about 112 m water depth (Figure 3a). The acoustic instrumentation was deployed at a depth of 50 m below surface on September 29, 2010 and retrieved on September 28, 2011. This site is situated in an ice shear zone with the ice season typically spanning from October through August. A large polynya commonly forms near the site in May as the ice begins its breakup process. The high mobility of ice at this location allows profiling of a substantial cross-section of ice distance and features. Extremely deep keels are observed along with wide hummock fields and occasional multi-year ice. Information about the RADARSAT-2 data

used for analysis (June 9, 2011) and corresponding meteorological conditions is provided in Table 1, while Table 2 presents ice draft and ice feature statistics derived from the ULS data.

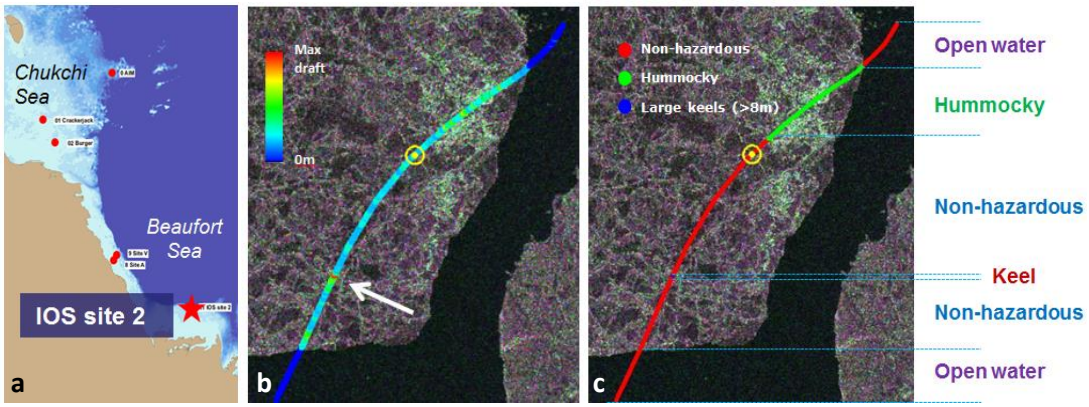

Figure 3. Beaufort Sea IOS site 2 dataset (June 9, 2011). (a) IOS site 2 mooring location. (b-c) The RADARSAT image is an RGB color composite of σ_{hh}, σ_{hv}, and σ_{vv}. The IPS track is colour coded by ice draft or hazardous ice type, where green is hummocky, blue is a deep keel, and red is water or ice that was not identified as hazardous.

Table 1. RADARSAT-2 data and meteorological conditions at the time of image acquisition[1]

Site	Date (yyyy-mm-dd)	Time (UTC)	Beam Mode	Direction	Air temp (°C)	Wind speed (m/s)	Wind direction[2] (°)
IOS site 2	2011-06-09	15:31:31	FQ20	Descending	-0.7	1.8	160

Table 2. Ice statistics for segments of ULS data corresponding to RADARSAT-2 data.

Site ID	Start	End	Mean Ice draft (m)	Max Ice draft (m)	Total distance (km)	% Hazardous Ice type		
						Non-hazardous	Keels (>8m)	Hummocky
IOS site 2	2011/06/09 12:03:19	2011/06/09 18:33:35	1.5	8.4	6.1	74.0	0.4	25.6

Qualitative assessment of polarimetric image products

The RGB color composite of HH, HV, and VV backscatter in Figure 3b-c shows the study area to consist of a rather dark floe, with a brighter area in the northeast that was identified by the IPS algorithm as hummocky ice (green section of the track in Figure 3c). A number of fine linear features, likely ridges, crisscross the floe. These were not characterized as hazardous (i.e., 8m keels or hummocky) by the IPS feature detection algorithms. Selected polarimetric products showing these features to a greater or lesser extent are illustrated in Figure 4. Based on visual inspection, products containing the most information are: Coherency matrix elements (T), Total power (span), Eigenvalues (λ_n), Shannon entropy, odd and volume scattering from Freeman-Durden and Yamaguchi decompositions. Other products that differentiated the hummocky area and open water but lacked finer detail included: Entropy (H), Alpha angle (α), Touzi alpha (α_s), polarization asymmetry and polarization fraction.

[1] Sources of meteorological data: IOS site 2 - Pelly Island (wind) & Tuktoyaktuk (air temp).
[2] Wind directions are given as direction TO.

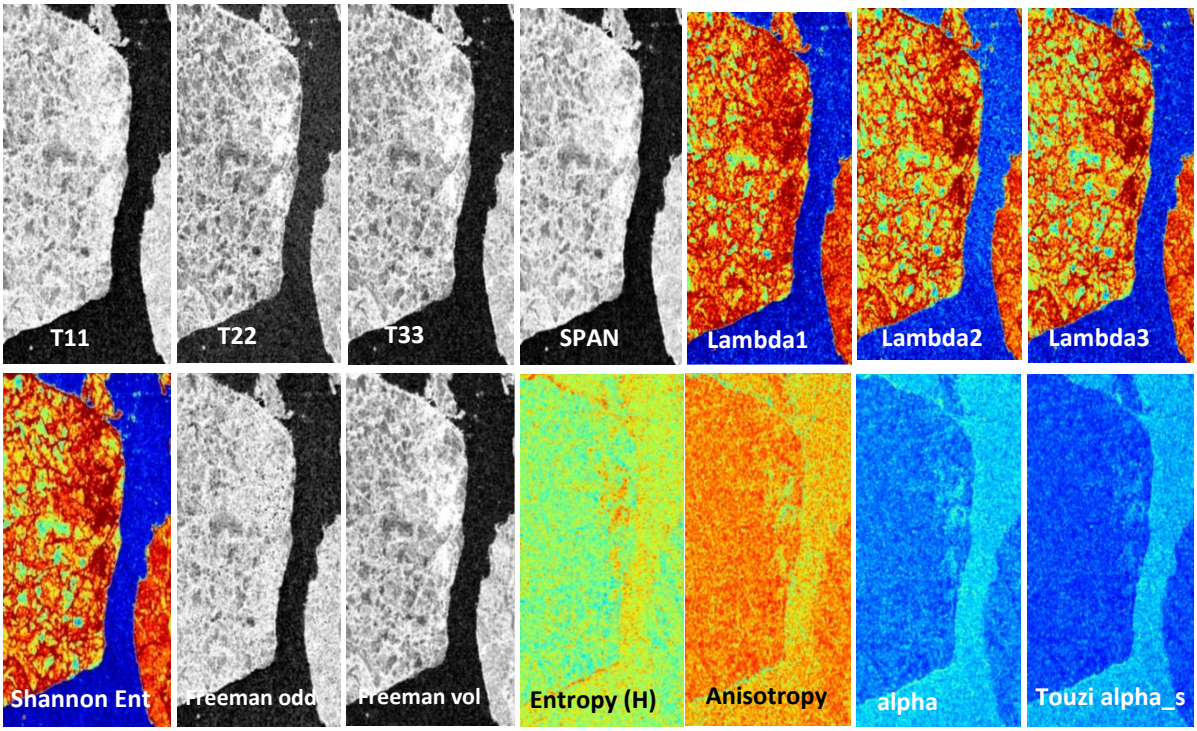

Figure 4. Selected polarimetric image products for the IOS site 2 dataset (9 Jun 2011)

Correlation of SAR Backscatter and Polarimetric Products with Ice Draft

Figure 5 compares spatial profiles of IPS ice draft with mean backscatter (σ_0) extracted from the imagery using kernel sizes ranging from 5x5m (single pixel) to 50x50m, where IPS draft was averaged to the same spacing as the image kernels in each plot. At the highest resolution there is little correspondence between IPS draft and backscatter, other than perhaps a generalized increase in signal level in the hummocky vs non-hazardous ice areas. We interpret the lack of correlation at high resolution in terms of a spatial mismatch between ice surface and bottom features: in a given area surface ridges and bottom keels may not mirror one another on a one-to-one basis, however in general they should both reflect a common scale of deformation. This in fact was what we observed: the correspondence between draft and backscatter improved with increasing kernel size (Figure 6a). Although image extracts larger than 350x350m were not evaluated, we expect that at some scale the correlation between draft and backscatter would begin to decrease. The scale of optimum correlation will vary with the scale of the ice features and with IPS/image misregistration.

As an example, for the one deep keel present in this dataset, the correspondence between IPS and backscatter was better at higher spatial resolutions (Figure 5b, Figure 6b). At coarse resolution the keel feature was overly smoothed and the correlation decreased. This effect of scale reveals an inherent limitation of using ice draft as validation for SAR ice thickness algorithms: even for robust SAR algorithms the strength of any correlation is limited by the correspondence of surface and bottom features and the scales at which they occur. However, it should still be possible to compare correlations for different SAR algorithms.

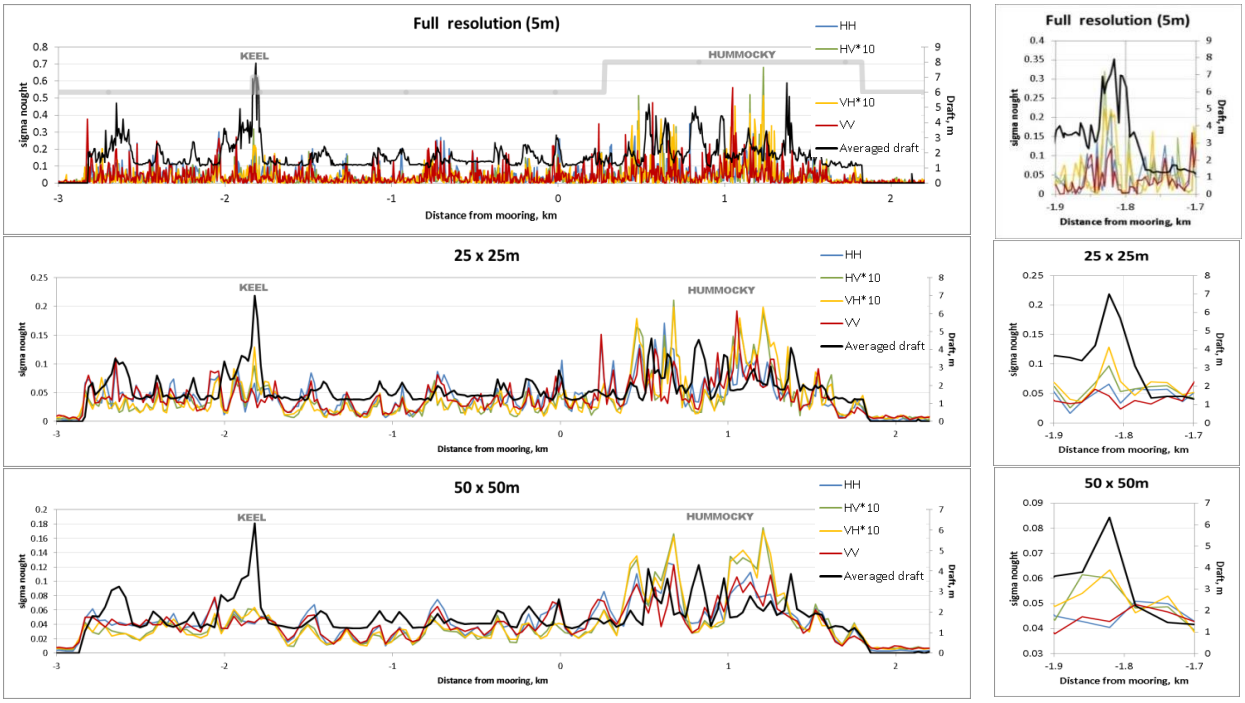

(a) (b)

Figure 5. (a) Comparison of ice draft measured by IPS (black) and σ_0 values averaged over kernel sizes of 5, 25, and 50m. Extents of hummocky and keel features identified from IPS are indicated by the grey line in the top plot. (b) Close-ups of the profiles over the deep keel.

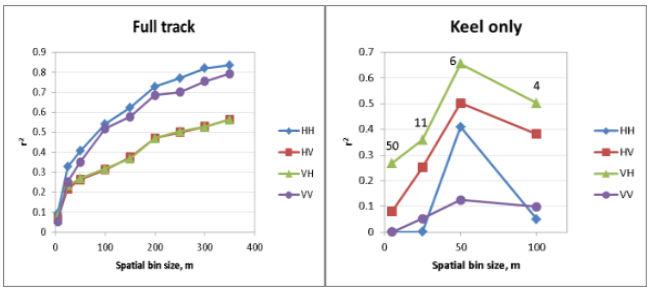

(a) (b)

Figure 6. Relationship of r^2 between ice draft and backscatter with spatial spatial bin size calculated over (a) the entire IPS track; (b) only over the keel segment. Labels on the keel plot show the number of data points (n) for each bin size.

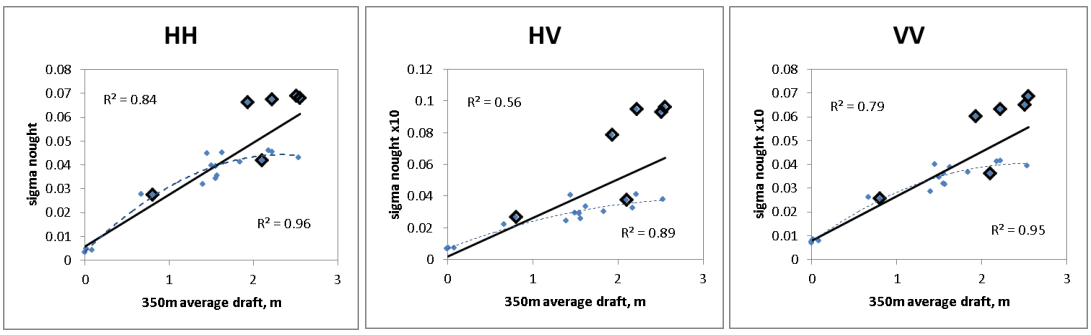

(a) (b) (c)

Figure 7. Scatterplots between 350m average ice draft and SAR backscatter (a) HH; (b) HV; (c) VV.

Figure 7 shows the scatterplots of ice draft vs SAR backscatter for 350m kernel size. Since cross-polarized backscatter channels HV and VH are very similar, only HV is shown. Dark outlined points are from the hummocky ice area based on IPS analysis. The r^2 values reported on the top left corner of the graphs are based on a linear fit to all of the data points (i.e., 0.84 for HH, 0.56 for HV, and 0.79 for VV). The values reported on the lower right corner are based on a curved fit to the non-hummocky ice only (i.e., 0.96, 0.89, and 0.95 for HH, HV, and VV, respectively). From these results a number of observations could be made:

- Hummocky ice often had stronger backscatter than non-hummocky ice. Conversely, pixels with elevated backscatter were associated with areas of hummocky ice. This was particularly true for cross-polarized channels (HV, VH). The stronger elevation of cross-polarized backscatter over hummocky ice may also explain the lower overall correlation with ice draft. Similarly, over the deep keel, elevation of the cross-polarized backscatter is stronger than the co-polarized channels (Figure 5b).
- For non-hummocky ice, there appeared to be a curved relationship between draft and backscatter, with backscatter values becoming saturated beyond about 2m of average ice draft (shown by dashed trend lines in Figure 7). The strength of this relationship was similar for all polarizations, slightly lower for cross-pol than co-pol.

A similar analysis of ice draft correlations with all polarimetric products suggested that, the ones that were highly correlated with ice draft (r^2>0.8 with 350m kernels) were in most cases the same as those that had been visually assessed to contain the most information. These were: the coherency matrix components, span, Shannon entropy, odd and volume scattering components of both Freeman-Durden and Yamaguchi decompositions. For polarimetric products that were highly correlated with ice draft, the relationships tended to be linear when all of the data points were used, and curved when hummocky ice was excluded.

For other datasets analyzed curved relationships were observed (no hummocky ice was present and also the average ice drafts were higher). We postulated that the relationships should in general be curved, with the digital number (DN) values for the polarimetric products saturating at some draft value that varies between polarimetric products. A recent study also reported saturation behavior between span and ice thickness (Casey *et al.*, 2013).

SAR classification

Polarimetric SAR classification algorithms available through open source software tools such as PolSARPro and RSTB (RADARSAT Toolbox) were evaluated in terms of their ability to approximate the ice feature classes as identified by the ULS data. The classification techniques tested were based on entropy, alpha angle and anisotropy or lambda, or Wishart unsupervised classification. Segmentation based on entropy, anisotropy and alpha angle (H/A/alpha) is a theoretical algorithm described by Cloude and Pottier (1997) that based on the scattering properties of the target, in this case sea ice. No statistical clustering is performed. Similarly H/alpha/lambda uses predetermined segmentation of these three parameters to classify ice type. The Wishart classification scheme performs a Maximum Likelihood (ML) statistical clustering of the polarimetric data set based on the multivariate complex Wishart probability density function of the Coherency Matrix (T3). A sub-optimal solution consists in optimizing this function using an iterative k-mean clustering algorithm that could be highly sensitive to the initialisation conditions. Lee *et al.* (1999) and Pottier *et al.* (2000) found that an initialisation using the results of the H/alpha and H/A/alpha segmentation procedure led to satisfying and stable results. Wishart classification seeded by Freeman Durden decomposition is first introduced by Scheuchl *et al.* (2005).

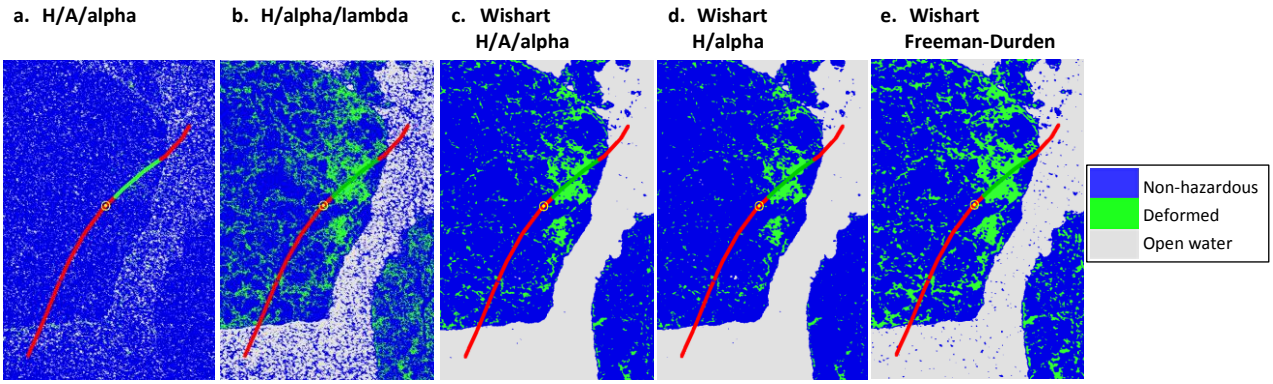

Figure 8. Classification results from standard (a) H/A/alpha and (b) H/alpha/lambda segmentations and Wishart unsupervised classifications seeded with (c) H/A/alpha, (d) H/alpha or (e) Freeman-Durden decomposition products.

The results from all datasets were similar, and indicate that the polarimetric parameters used contain information for the discrimination of (ULS-defined) ice types. Individual classification algorithms varied in their capability to extract this information. Results for the IOS site 2 dataset are shown in Figure 8 and Table 3.

Findings for specific classification algorithms were:

- Standard H/A/alpha segmentation (Figure 8a) achieved little or no separation of ice classes.
- Segmentation based on H/alpha/lambda (Figure 8b) greatly improved the separation of ice classes and open water.
- Wishart clustering with H/A/alpha seeding (Figure 8c) improved classification results relative to standard segmentation using the same parameters without clustering (Figure 8a).
- Excluding anisotropy (A) from the Wishart seeding (Figure 8d) had variable results depending upon the dataset.
- Hazardous ice was identified by all classifiers except for standard H/A/alpha.
- The best overall accuracy was achieved using Wishart clustering seeded with any of the parameter sets tested.
- The highest classification accuracy for deformed ice was obtained with Freeman-Durden seeding. H/alpha or H/A/alpha seeding resulted in underestimates of deformed ice. Because the classifications tended to include the fine ridging visible in Figure 3, as well as the hummocky ice detected by ULS, this class is referred to as deformed ice in Figure 8 and Table 3.

Work in progress

The polarimetric data analysis has since been extended to compact polarization (CP) using simulated CP dataset. An initial assessment of the CP mode was performed with comparison to the quad-pol analysis. In addition to the ongoing development of improved classification and draft estimation algorithms, a winter dataset from NE Greenland, where MYI is present, has been analyzed.

Table 3. Accuracy assessment of selected classifiers using IPS classification for validation.

H A alpha segmentation	Non-hazardous	Deformed	Open water	Producer's Accuracy
Non-hazardous	801	2	58	93.0%
Hummocky	295	6	32	1.8%
Open water	264	6	85	23.9%
User's Accuracy	58.9%	42.9%	48.6%	**57.6%**

H alpha lambda segmentation	Non-hazardous	Deformed	Open water	Producer's Accuracy
Non-hazardous	726	122	13	84.3%
Hummocky	123	210	0	63.1%
Open water	93	0	262	73.8%
User's Accuracy	77.1%	63.3%	95.3%	**77.3%**

H A alpha seeded Wishart	Non-hazardous	Deformed	Open water	Producer's Accuracy
Non-hazardous	816	35	10	94.8%
Hummocky	139	194	0	58.3%
Open water	9	0	346	97.5%
User's Accuracy	84.6%	84.7%	97.2%	**87.5%**

H alpha seeded Wishart	Non-hazardous	Deformed	Open water	Producer's Accuracy
Non-hazardous	836	15	10	97.1%
Hummocky	157	176	0	52.9%
Open water	8	0	347	97.7%
User's Accuracy	83.5%	92.1%	97.2%	**87.7%**

Freeman-Durden seeded Wishart	Non-hazardous	Deformed	Open water	Producer's Accuracy
Non-hazardous	752	100	9	87.3%
Hummocky	94	239	0	71.8%
Open water	10	2	343	96.6%
User's Accuracy	87.9%	70.1%	97.4%	**86.1%**

CONCLUSIONS

In this paper, we presented an overview of our ongoing R&D efforts to characterize hazardous ice conditions using Upward Looking Sonar and spaceborne SAR data, where we aimed to enhance ice information products by combining the "view from above" with the "view from below".

High resolution and quad-polarized data from RADARSAT-2 and ice draft and velocity data from ULS moorings in the Beaufort the Chukchi and NE Greenland were analyzed. Methodologies were developed for validation of satellite-based ice information products using the upward looking sonar data. SAR classification methods were assessed for ULS-based hazardous ice types and ice draft was estimated from SAR datasets. The results from one dataset in the Beaufort Sea (IOS site 2) were presented.

To allow co-registration of satellite and ULS datasets for comparison and validation purposes, one of the main limiting factors is the requirement of spatially coherent ice motion with no significant deformation. For "correlation length" (the extent that two datasets spatially correlate) assessment image-based ice velocity field or correspondence of distinct features (e.g., floe edges) in the imagery and ULS data are used. In the process of assessing the correlation length, it was found that sometimes limited accuracy of the ice velocity direction information may result in an apparent rotation of the IPS track image overlay. This is attributed to the characterization of ADCP compass calibration (typically is not a limiting factor for studies based on ULS datasets).

The results of our analysis on datasets from the Beaufort and the Chukchi Seas suggest that there is some variability in the ability of SAR polarimetry to estimate ice draft or detect hazardous ice features, as measured by ULS. The three types of assessments including the visual assessments of RADARSAT-2 scenes, and the results of draft correlations and histogram analyses, several of the products were consistently better than others. These include the components of T3 coherency matrix, total power (span), Eigenvalues (λ_n), Shannon entropy, and Freeman-Durden volume scattering. Other products were variable among assessments and/or among datasets. In general, our observations were in agreement with a recent study (Gill *et al.*, 2013) where classification potential for different first year ice types was assessed based on probability density functions. They have reported high classification potential for some of these products as well as variability between datasets. For polarimetric products that showed good correlations with ice draft, the relationships in general were curved, with the polarimetric products saturating at some ice draft value. This is consistent with a recent study, where *in situ* and airborne measurements of multiyear sea ice thickness were compared with polarimetric SAR data (Casey *et al.*, 2013).

ACKNOWLEDGEMENTS

The funding and RADARSAT-2 data for this work were provided by the Canadian Space Agency Earth Observations Application Development Program (CSA - EOADP). The permissions to use upward looking sonar (ULS) datasets were granted by the owners and their program partners that include the Department of Fisheries and Oceans Canada (DFO) and NOAA; Shell Oil; and Statoil and NTNU (Norwegian University of Science and Technology).

REFERENCES

Casey, J.A., J. Beckers, T. Busche and C. Haas, 2013. Comparison of *in situ* and airborne measurements of multi-year sea ice thickness with dual-frequency, polarimetric SAR observations. Proc. IGARSS 2013.

Cloude, S.R., and E. Pottier, 1997. An entropy based classification scheme for land applications of polarimetric SAR. IEEE TGRS, Vol. 35, No. 1, pp. 68_78.

Fissel, D.B. and J.R. Marko, 2011. Understanding the changing Arctic sea ice regime. Essay in: J. Ocean Technology, Vol. 6(3), October 2011.

Fissel, D.B., E. Ross, K. Borg, D. Billenness, A. Kanwar, A. Bard, D. Sadowy, and T, Mudge, 2012. Improvements in the detection of hazardous sea ice features using Upward Looking Sonar Data, Arctic Technology Conference, 2012.

Fissel, D.B, J.R. Marko and H. Melling, 2008. Advances in Marine Ice Profiling for Oil and Gas Applications," Proceedings of the Icetech 2008 Conference, July 2008.

Freeman, T., and Durden, S.L. 1998. A three-component scattering model for Polarimetric SAR data. IEEE Trans. of Geoscience and Remote Sensing, Vol. 36, No. 3, pp. 963_973.

Gill, J.P.S. and J.J. Yackel, 2012. Evaluation of C-band SAR polarimetric parameters for discrimination of first-year sea ice types. Can. J. Rem Sensing Vol 38, No. 3,pp.306-323.

Gill, J.P.S., J.J. Yackel and T. Geldsetzer, 2013. Analysis of consistency in first-year sea ice classification potential of C-band SAR polarimetric parameters. Canadian Journal of Remote Sensing Vol 39, no. 2.

Kim**,** J-W., D-J. Kim, and B.J. Hwang, 2012. Characterization of Arctic Sea Ice Thickness Using High-Resolution Spaceborne Polarimetric SAR Data, IEEE Trans. on Geoscience and Remote Sensing, Jan 2012.

Lee, J-S., M.R. Grunes, T.L. Ainsworth, L.J. Du, D.L. Schuler, and S.R. Cloude, 1999. Unsupervised Classification using Polarimetric Decomposition and the Complex Wishart Distribution, IEEE TGRS, 37(5).

Pottier,E., J-S Lee, Unsupervised classification scheme of POLSAR images based on the complex Wishart distribution and the 'H/A/alpha' polarimetric decomposition theorem EUSAR 2000, 265-268.

Scheuchl, B., I. Hajnsek, and I.G. Cumming, 2003. Classification strategies for fully polarimetric SAR data of sea ice. Proc. POLinSAR, Frascati, Italy, 14-16 January, 2003.

Scheuchl, B., I.G. Cumming, and I. Hajnsek, 2005. Classification of fully polarimetric single- and dual-frequency SAR data of sea ice using the Wishart statistics, Can. J. Rem. Sens., Vol.31, No. 1.

Touzi, R., 2007. Target scattering decomposition in terms of roll-invariant target parameters. IEEE Trans. on Geoscience and Remote Sensing, Vol. 45, No. 1, pp. 73_84.

Yamaguchi, Y., T. Moriyama, M. Ishido and H. Yamada, 2005. Four-component scattering model for polarimetric SAR image decomposition. IEEE Trans. on Geoscience and Remote Sensing, Vol.43, No.8.